

Lawrence Berkeley National Laboratory

Lawrence Berkeley National Laboratory

Title

Time Resolved Shadowgraph Images of Silicon during Laser Ablation: Shockwaves and Particle Generation

Permalink

<https://escholarship.org/uc/item/4pz9v364>

Authors

Liu, C.Y.
Mao, X.L.
Greif, R.
et al.

Publication Date

2006-05-06

Peer reviewed

Time Resolved Shadowgraph Images of Silicon during Laser Ablation: *Shockwaves and Particle Generation*

C Y Liu, X L Mao, R Greif, R E Russo*

Lawrence Berkeley National Laboratory, Berkeley, CA 94720, USA

*Corresponding author. Tel.: +1-510-486-4258; fax: +1-510-483-7303.

E-mail address: rerusso@lbl.gov

Abstract. Time resolved shadowgraph images were recorded of shockwaves and particle ejection from silicon during laser ablation. Particle ejection and expansion were correlated to an internal shockwave resonating between the shockwave front and the target surface. The number of particles ablated increased with laser energy and was related to the crater volume.

1. Introduction

The growing interest of laser ablation is seen in various applications including chemical analysis¹, nano-material generation² and micromachining³. Aerosol particles generated from laser ablation vary from several nanometers to several tens of micrometers in diameter depending on the incident laser energy⁴, ambient pressure⁵, and sample material⁶. Mechanisms of particle generation as well as their relation to operating parameters need to be understood for optimizing various applications. The dynamics of vapor plume propagation and the shockwave are critical in determining the temperature and pressure that facilitate aerosol formation. Nanometer diameter particles most likely form from condensation when the high temperature vapor plume cools during its expansion into an ambient gas. Other particle generation mechanisms can occur including exfoliation (thermal induced stress fracture), which involves solid fragments that are ejected from the sample, and spallation, which involves particles that are ejected from the molten pool⁷. These particles are larger in size (hundreds of nanometers to several microns) and can be discerned by their shape. Particles ejected from the solid state have irregular shapes whereas particles ejected from the molten pool establish a spherical shape due to surface tension.

Significant changes in the quantity of mass ablated are observed as the laser irradiance crosses various threshold values; the ablation rate is usually a nonlinear function of laser irradiance⁹. Large particle ejection normally accompanies the increased ablated mass. Several mechanisms have been reported to describe this particle ejection process. As the vapor plume and shockwave expand, recoil pressure interacts with the molten surface causing a raised rim around the crater and ejection of liquid droplets. At very high laser irradiances, explosive boiling, or phase explosion⁸ also is responsible for generating large craters and large solid particles. In this paper, these two mechanisms (recoil pressure and explosive boiling) were studied by measuring time resolved shadowgraph images during ablation of silicon samples. A resonating internal shockwave is proposed as the driving force that causes molten particles to eject from the sample surface.

2. Experimental system and method

The experimental system included two lasers: a Nd:YAG (266 nm wavelength with 4 ns pulse duration, New Wave Research, Tempest 10) for ablation and a Ti: sapphire (800 nm wavelength with 150 fs pulse duration, Spectral-Physics) for imaging. The pulse timing between the two lasers was controlled via a delay generator (Stanford DSG 535). Laser fluence was varied by controlling the laser beam energy and ensuring a constant focal spot diameter (~70-micron spot diameter on the sample surface using a single lens). Silicon was used as the sample and placed in atmospheric pressure air. Each shadowgraph image was measured for ablation with a single laser shot on a fresh Si sample surface. The image size is approximately 500 microns in the distance from the target surface. After ablation, the depths of the laser-ablated craters were measured using a white-light interferometric microscope (New View 200, Zygo).

3. Results

3.1. Shadowgraph images of silicon ablation

Time-resolved shadowgraph images measured during ablation of silicon with different laser energies are shown in Figure 1. Using a laser energy of 0.4 mJ, plume expansion and shockwave propagation were observed, but particles were not ejected from the surface (Figure 1 a). For 6mJ of laser energy, particle ejection from the surface was observed after the vapor plume and shockwave expansion (Figure 1 b). Unlike most materials⁹⁻¹² in which particles were ejected at an angle to the surface normal, particles ejected from silicon were perpendicular to the surface. The stream of ejected Si particles resembled that of a liquid jet and lasted for ~2 microseconds after the laser pulse. At ~2 microseconds after the laser pulse, larger irregular shaped particles were observed. These particles are believed to originate from the solid phase as evidenced by their irregular shape. The ejection of these particles lasts for 50 microseconds after the laser pulse.

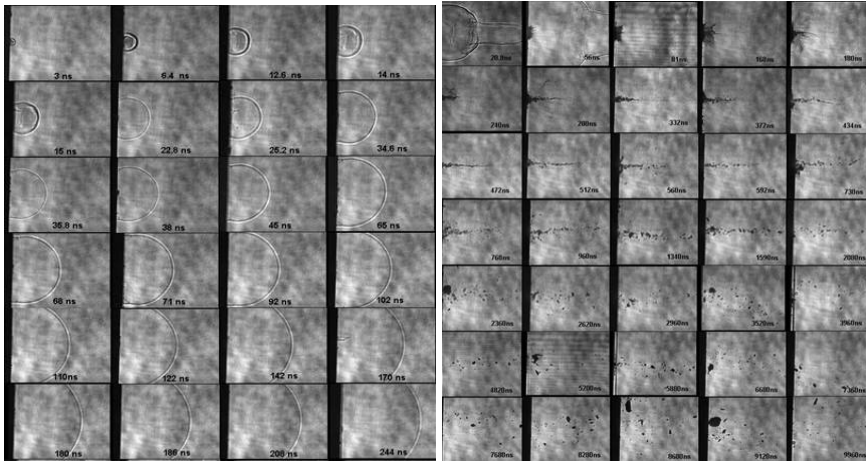


Figure 1. (a) Shadowgraph images from ablation on silicon at 0.4 mJ (b) Shadowgraph images from ablation on silicon at 6 mJ

3.2. Effects of Internal Shockwaves

From a copper surface at a laser energy of 12mJ, our measured time resolved images show that an internal shockwave exists and that it clearly changed shape with time as it traveled toward and then reflected from the surface (Figure 2a). The existence of internal shockwaves and their effects on the ablation processes have been discussed in the literature^{13,14}. Particle ejection occurred after the secondary shockwave reflected from the surface. Although the profile of particle ejection of copper and silicon is different, the mechanism of the internal shockwave should be similar.

Figure 2b shows time resolved images during ablation of silicon at the same laser energy. The internal shockwave was observed first at 7ns after the laser pulse. At this time the front of the internal

shockwave was still in contact with the vapor plume. The center of the internal shockwave then moved inward (10 ns) and eventually exhibited a U-shape (44ns) as it separated from the vapor-plume front. The particle plume was observed as early as 20ns and could be caused by the internal shockwave acting on the molten surface. The ejection speed of these particles was obtained from the images and is shown in Figure 3. The internal shockwave again was observed at 44ns and reached the surface at 52ns. The jet stream of particles appeared at 52ns and had a speed of ~ 900 m/sec (Figure 3); the shockwave speed was much faster than the particle speed. The speed of the external shockwave was obtained from the first two images in Figure 2b to be about 4000 m/sec. The liquid jet initially moved as a narrow stream into the air ambient. The image at 94 ns shows branching of the jet stream, which could be due to its interaction with the internal shockwave. The internal shockwave can resonate within the vapor plume being reflected from the target surface and shockwave front, influencing the ejection and expansion of particles. Unlike copper, secondary shockwaves (at later times) could not be observed due to ejection of the liquid silicon jet perpendicular to the surface. The difference in the angular direction of particles from Cu and Si could be caused by the effective instability on the surface produced by the resonating internal shockwave¹⁵.

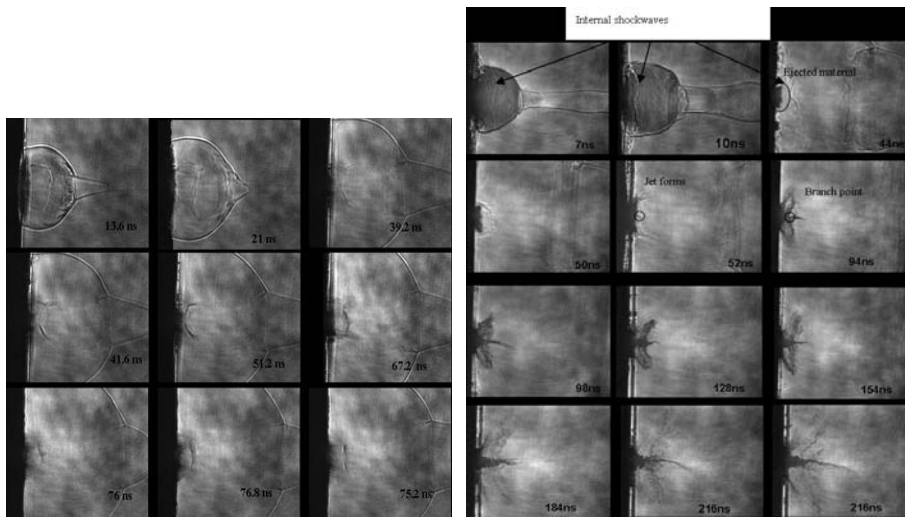


Figure 2. Internal shockwave from ablation at 12mJ (a) on copper (b) on silicon

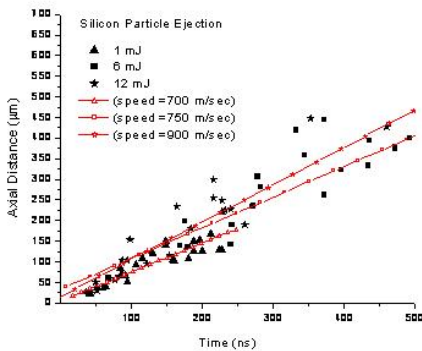


Figure 3. Trajectory of front position of silicon particles. The hollow legend with line is the fitting result of the data, the slope represents the speed of the particles.

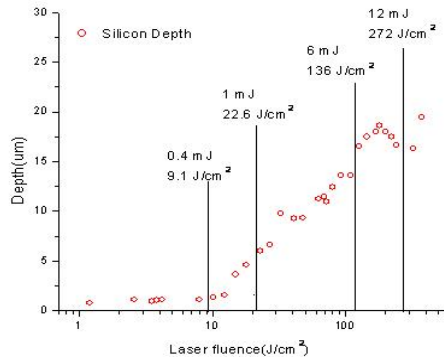


Figure 4. Ablation rate for copper and silicon at different laser fluence

3.3. Change in ablation mechanism with laser energy

Figure 4 shows the measured crater depth in silicon versus laser fluence. Shadowgraph images were recorded at four laser energies (and corresponding fluences). The crater depth data and the

shadowgraph images were consistent in showing different processes. The crater depth was less than 1 micron for when the energy was below 0.4mJ, then increased sharply starting at ~0.5mJ and plateaued at roughly 8mJ. The increased crater depth coincided with changes in particle ejection as observed in the shadowgraph images. At low laser energy, vaporization is likely a dominant mechanism for mass removal; the vapor plume and shockwave were observed but not particles. The jet stream of silicon particles as well as the internal shockwaves was observed when the laser energy was greater than 1mJ (not shown). A theoretical simulation¹⁶ demonstrated that the maximum melted region (~3 microns at a 6 mJ laser energy) occurred at ~50 ns after the laser pulse, which was approximately the time it took the internal shockwave to hit the surface. The melt thickness remains larger than 1 micron until 1.5 microseconds after the laser pulse, the duration of the melt supports liquid jet formation until ~1 microsecond after the laser pulse.

Melt-flushing due to the internal shockwave can be a mechanism to describe the jet stream of particles but not the larger craters and particles produced at higher laser fluences. Yoo⁹ reported that the bottom of the crater was smooth at low laser irradiance and became rough at higher irradiance. The change in crater roughness combined with the abrupt change in crater volume when the laser irradiance was higher than a “threshold” value was attributed to phase explosion. From the shadowgraph images at high laser energies (>6 mJ), large solid particles were ejected after ~2 microsecond (particles were irregular shape and deviated from the jet stream particles). These large solid particles, though small in number, make up a significant portion of the ablated mass. A rough crater bottom supports the hypothesis that mass removed was in the solid phase; otherwise surface tension would result in a curved smooth profile if the surface was in the molten state. At high laser fluence, thermal induced stress surpasses the mechanical strength and cause exfoliation.

4. Summary

During ablation with high laser irradiance, particle ejection can occur from numerous mechanisms. For silicon, particle ejection resembled a liquid jet with a narrow divergence whereas copper particles were broadly dispersed. The ejection and divergence was related to the interaction of an internal shockwave applying pressure on a molten surface. At ~1.5 microsecond after the laser pulse, and for greater fluences, large particles were ejected in solid form and composed a significant portion of the mass removed. These larger particles were ejected by exfoliation and phase explosion processes. The quantity of the mass ablated increased non-linearly with the laser energy and was correlated to the measured crater volume.

Acknowledgments

The US Department of Energy, Office of Basic Energy Sciences, Division of Chemical Sciences, and the Office of Nonproliferation and National Security (NA22) supported this research at the Lawrence Berkeley National Laboratory under Contract No. DE-AC02-05CH11231

Reference

- [1] Russo R E, Mao X L, Borisov O V 1998 *Trac-Trends in Analytical Chemistry* **17** 461
- [2] Zhang Y, Chen WZ, Zhang WG 2003 *Chemical Journal of Chinese Universities-Chinese* **24** 337
- [3] Ritsko J J 1989 *Laser Micro-Fabrication: Thin Film Processes and Lithography*. San Diego: Academic
- [4] Jeong S H, Borisov O V, Yoo J. H, Mao, X L Russo, R E 1999 *Analytical Chemistry* **71** 5123
- [5] Gnedovets, A G, Gusarov, A V, Smurov I 2000 *Applied Surface Science* **154-155** 508
- [6] Ozawa E, Kawakami Y, Seto T 2001 *Scripta Mater* **44** 2279
- [7] Webb R L, Dickinson J T, Exarhos G J 1997 *Appl Spectrosc* **51** 707
- [8] Yoo J H, Jeong S H, Greif R, Russo R E 2000 *J. Appl. Phys* **88** 1638
- [9] Angleraud B, Garrelie F, Tetard F, Catherinot A 1999 *Applied Surface Science* **139** 507
- [10] Hopp B, Kresz N, Vass C, Toth Z, Smausz T, Ignacz F 2002 *Applied Surface Science* **186** 298

- [11] Voisey K T, Kudesia S S, Rodden W S O, Hand D P, Jones J D C 2003 *Mater. Sci. Eng* **356** 414
- [12] Hauer M, Funk D. J, Lippert T, Wokaun 2004 *Thin solid films* **453-454** 584
- [13] Anisimov S I, Bauerle D, Lukyanchuk B S 1993 *Physical Review B* **48** 12076
- [14] Arnold N, Gruber J, Heitz J 1999 *Appl. Phys. A* **69** S87
- [15] Wen S, Liu, C. Y 2005 Ongoing work from our lab